A Supply Voltage Insensitive Two-Transistor Temperature Sensor with PTAT/CTAT Outputs based on Monolithic GaN Integrated Circuits

Ang Li, *Student Member, IEEE*, Fan Li, Kaiwen Chen, Yuhao Zhu, Weisheng Wang, Ivona Z. Mitrovic, *Senior Member, IEEE*, Huiqing Wen, *Senior Member, IEEE*, and Wen Liu, *Member, IEEE*

***Abstract*—The paper presents a monolithically integrated temperature sensor using a two-transistor (2T) configuration based on gallium nitride (GaN) metal–insulator–semiconductor high-electron-mobility transistors (MIS-HEMTs). By adjusting the gate size ratio of the depletion-mode (D-mode) device and enhancement-mode (E-mode) device, the output type of the sensor can be converted between proportional to absolute temperature (PTAT) and complementary to absolute temperature (CTAT). Experimental results demonstrate that the 2T configuration achieves PTAT/CTAT output with high temperature sensitivity (PTAT/CTAT: 15.86/−10.53 mV/°C) over a wide temperature range of 25 to 250 °C and a broad supply voltage range of 8 to 60 V, attributed to the superior characteristics of the GaN transistor. Additionally, the integrated over-temperature protection (OTP) block based on this temperature sensor has been fabricated in the laboratory, which features a fast response time (381 ns at 150 °C). These results demonstrate the viability of on-chip integrated sensors in OTP circuits that are fully compatible with 48 V applications and a high-temperature environment, paving the way for the development of high-power density all-GaN smart power systems.**

***Index Terms*—GaN, monolithic integration, temperature sensor, over-temperature protection, PTAT, CTAT.**

I. Introduction

GALLIUM nitride has huge potential in power conversion applications due to its superior high breakdown, high temperature and fast switching characteristics [1], [2], [3]. Especially in electric vehicles, GaN brings a solution to high operating temperatures, and the inherent thermal properties mitigate the demand for cooling systems [4], [5]. However, high-temperature sensing is still required for safe operation and reliable system thermal control.

Sensitivity is a key parameter for on-chip temperature sensors in over-temperature protection circuits, but the previous GaN on-chip approaches achieved limited performance. GaN-based Schottky barrier diodes (SBDs) have exhibited remarkable temperature sensing capabilities, with an operating temperature of up to 250 °C and a sensitivity of 2.25 mV/K [6]. To further enhance sensitivity, additional metallic materials such as Ni and TiN are used [7], resulting in more process steps and masks. The two-dimensional electron gas (2DEG) resistor can also be employed as a temperature sensor in power devices at temperatures exceeding 200 °C [8], but with limited sensitivity. Monolithic integration of GaN temperature sensing can be accomplished with a current mirror and ring oscillator structure [9], [10], which offers a broad temperature range and good sensitivity. However, these circuits are only capable of operating at a certain supply voltage and require more than 10 transistors. To ensure proper protection, it is necessary to design temperature sensors with the flexibility to use CTAT or PTAT [10], [11].

In this paper, we demonstrate an integrated GaN temperature sensor with two transistors based on the MIS-HEMT technology platform. The experimental investigation of on-chip temperature sensing is reported to enhance sensitivity over a wide temperature range and offers a tunable PTAT/CTAT state. Furthermore, this sensor exhibits integrated over-temperature protection function availability. The high temperature and supply voltage tolerance of this sensor, which is based on GaN technology, makes it suitable for a variety of application scenarios, including 48 V applications [12].

II. Operating Principle of Temperature Sensor

The integration of E-mode and D-mode GaN MIS-HEMTs enables the realisation of GaN ICs, which are applied to construct various peripheral circuits [13], [14]. The MIS-HEMTs structure is demonstrated in Fig. 1(a), which shows the GaN-on-Si platform with active and passive components. The fabrication processes are detailed described in [14]. Fig. 1(b) shows the transfer characteristics of the MIS-HEMT device at 25 °C and 250 °C. The D-mode device has a threshold voltage $V_{th,D}$ of −2.21 V at 25 °C and −2.09 V at 250 °C. The E-mode device shows a $V_{th,E}$ of 2.70 V at 25 °C and 2.85 V at 250 °C. The maximum variation in an E-mode device is 0.15 V, while the maximum variation for a D-mode device is 0.12 V, as shown in Fig. 1(c).

The basic structure of the proposed temperature sensor is shown in Fig. 2(a). The circuit comprises two transistors, M1 in D-mode and M2 in E-mode, connected in series. The gates of M1 and M2 are jointly connected to the drain terminal of M2, producing the output voltage V_{sen}. M1 has a gate-to-source voltage $V_{GS,1} = 0$ V, which works as a current source; The bottom transistor M2 has a gate-to-source voltage $V_{GS,2} = V_{sen}$, acting as a diode.

This work was supported by the National Key R&D Program of China (2022YFB3604400), the Suzhou Science and Technology program SYG202131, XJTLU Key Program Special Fund KSF-T-07, Research Development Fund RDF-20-02-43. (Corresponding authors: *Wen Liu*).

A. Li, F. Li, K. Chen, Y. Zhu, W. Wang, H. Wen, and W. Liu are with the Department of Electrical and Electronic Engineering, Xi'an Jiaotong-Liverpool University, Suzhou 215123, China; and also Department of Electrical Engineering and Electronics, University of Liverpool, Liverpool L69 3GJ, U.K. (e-mail: wen.liu@xjtlu.edu.cn)

I. Z. Mitrovic is with the Department of Electrical Engineering and Electronics, University of Liverpool, Liverpool L69 3GJ, U.K.

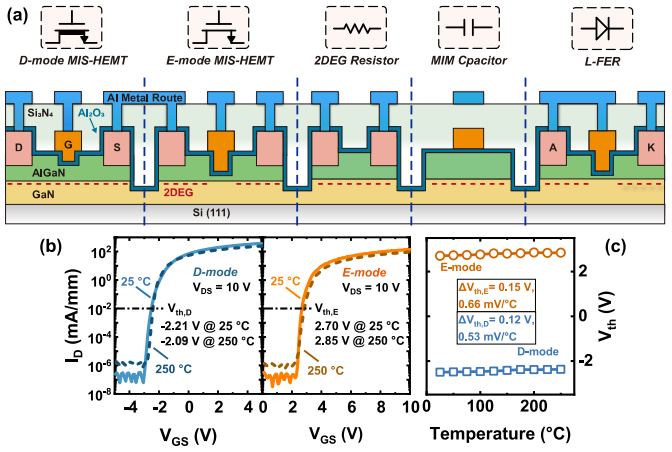

Fig. 1. (a) Schematic diagram of the GaN-on-Si platform based on MIS-HEMT technology. (b) Transfer characteristics of D/E-mode MIS-HEMTs at 25 °C (solid line) and 250 °C (dash line). (c) The threshold voltage V_{th} versus the various temperature from 25 to 250 °C.

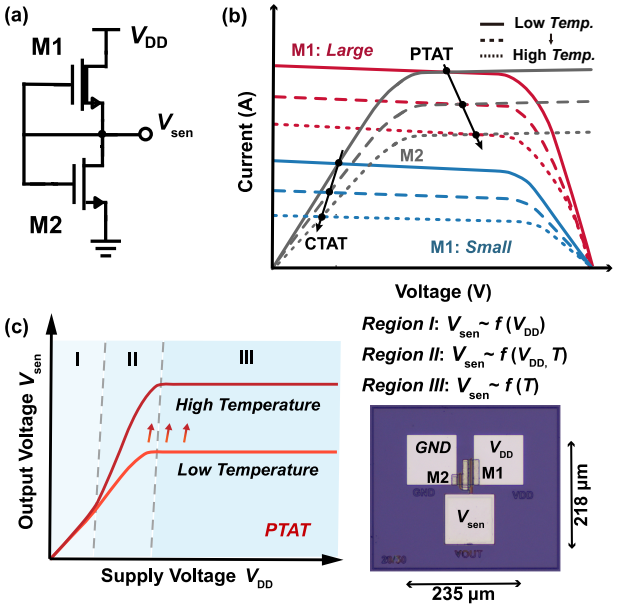

Fig. 2. (a) Circuit schematic of the 2T temperature sensor; and (b) I-V characteristics to form PTAT/CTAT state. (c) Schematic diagram of the generation of a PTAT with three operation regions, and the microphotograph of the fabricated PTAT-sensor (CTAT- has the same area).

The size ratio of transistors M1 and M2 determines whether the temperature sensor operates in a PTAT or CTAT mode (Fig. 2(b)). The output voltage is PTAT if M1 is larger than M2, while CTAT if M1 is smaller. For the sizes of M1/M2 used in this paper, gate widths are W_{M1}/W_{M2} = 20/50 μm (CTAT-sensor), 50/20 μm (PTAT-sensor), and gate length $L_{GS}/L_G/L_{GD}$ = 3/2/3 μm, respectively. The area of this temperature sensor structure is 0.051 mm^2, including the probe pads.

As the supply voltage increases from 0 V, the output voltage V_{sen} exhibits three distinct regions, as depicted in Fig. 2(c). In region I, the low supply voltage ensures that the drain-to-source voltage of M1 ($V_{DS,1}$) remains in the linear range, while M2 remains in cut-off mode, resulting in $V_{sen} = V_{DD}$.

With a minor increase in V_{DD} in region II, M1 remains in its linear mode while the 2T circuit conducts an increasing current, causing M2 to conduct. Due to the linear and non-saturated mode of operation, the output voltage V_{sen} is dependent on both V_{DD} and temperature T, as $V_{sen} \sim f(V_{DD}, T)$. Subsequently, as V_{DD} continues to rise into region III, M1 enters the saturation mode and operates as a constant current source. In this mode, M1 counteracts the increasing current flow, ensuring a stable output voltage that remains independent of variations in V_{DD}. This stable output voltage enables reliable operation of the two-transistor temperature sensor.

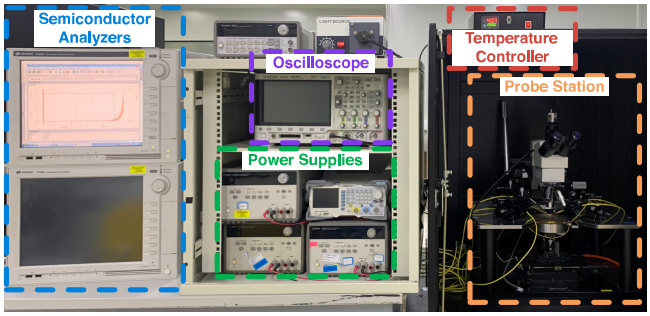

Fig. 3. Setup of the test platform for the temperature sensor.

The size ratio of M1 and M2 serves as the criterion for determining the PTAT or CTAT state based on the current operating match. When the size ratio is small, M2 operates in subthreshold mode ($V_{GS,2} = V_{sen} < V_{th,E}$), resulting in an output with a negative temperature coefficient, known as the CTAT state. In contrast, for a M1 size that is large enough, M2 operates in saturation mode ($V_{GS,2} = V_{DS,2} = V_{sen} > V_{th,E}$, $V_{DS,2}$ is the drain-to-source voltage of M2), leading to a positive temperature coefficient, as the PTAT state. The output voltage V_{sen} is dependent on the temperature T only, as $V_{sen} \sim f(T)$.

III. Characteristics of Temperature Sensor

The characteristics of the GaN temperature sensor were measured by Agilent 1505 power device analyser. The probe station was sealed off during testing to minimise ambient temperature drift. The test platform is shown as Fig. 3. Fig. 4(a) and (b) show the output voltage versus V_{DD}, at temperatures ranging from 25 to 250 °C (with 25 °C/step). The ability of the circuit to generate the PTAT and CTAT outputs has been demonstrated. The high drain voltage tolerance of GaN transistor M1 allows its operation in a wide supply voltage range from 8 to 60 V. The proposed on-chip GaN temperature sensor is compatible with power conversion circuits and is able to operate at extreme temperatures exceeding 200 °C contrast to Si CMOS, making it a promising candidate for use in electric vehicles, petroleum, and space electronics [4], [5].

Fig. 5(a) shows the sensing measurement results versus temperature, with a temperature sensitivity ($\Delta V_{sen}/\Delta T$) of 15.86 mV/°C and −10.53 mV/°C for the PTAT- and CTAT-based implementation, along with linearity of 0.992 and 0.989. Additionally, Fig. 5(b) shows the supply voltage sensitivity at the corresponding temperature. As temperature increases, the output curves maintain high immunity to supply voltage

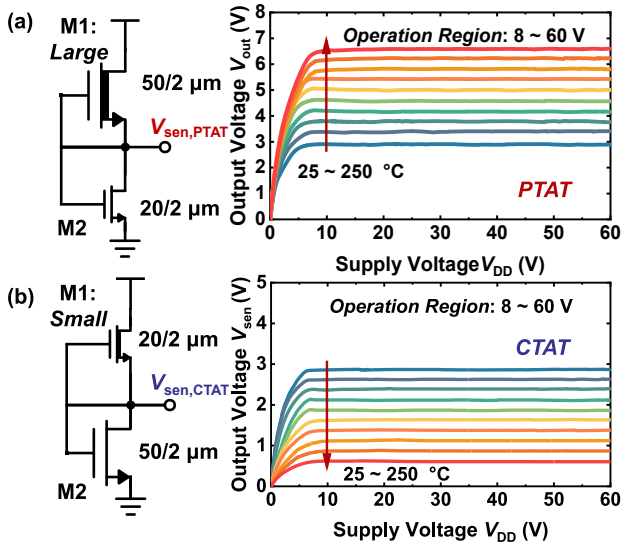

Fig. 4. Measured output voltage V_{sen} versus supply voltage V_{DD} for (a) PTAT-sensor and (b) CTAT-sensor.

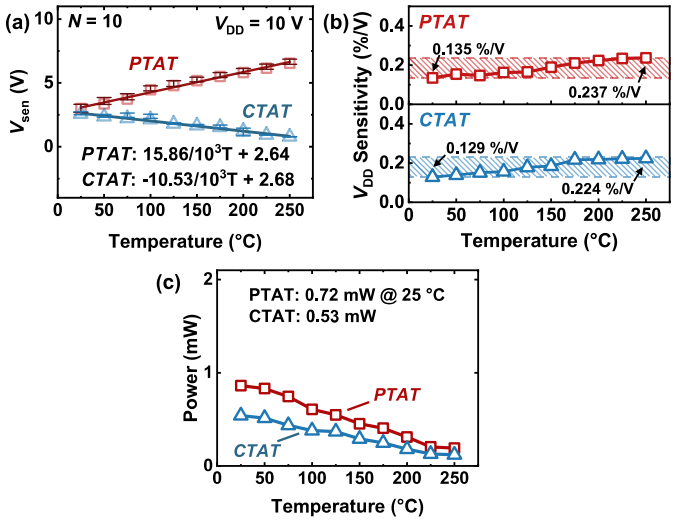

Fig. 5. (a) The sensor output performances versus temperature with error bars of 10 samples, as 15.86 ± 0.42 mV/°C (PTAT-sensor) and −10.53 ± 0.19 mV/°C(CTAT-sensor). (b) Supply voltage sensitivity at each temperature, with V_{DD} = 8∼60 V. (c) Power consumption of 2T sensors at V_{DD} = 10 V and 25 °C.

changes, achieving a maximum supply voltage sensitivity of 0.237 %/V of PTAT and 0.224 %/V of CTAT. The power consumptions of 0.72 mW (PTAT) and 0.53 mW (CTAT) at V_{DD} = 10 V are shown in Fig. 5(c).

In contrast to Si CMOS technology temperature sensing for low voltage applications, on-chip GaN temperature sensing is used for power conversion applications. Table I compares several implementations of the GaN temperature sensor. The proposed design of the monolithic integrated 2T sensor on GaN MIS-HEMT platform achieves a wider supply range (8∼60 V) and higher temperature sensitivity (15.86/−10.53 mV/°C), while occupying a smaller area (0.05 mm^2). A higher operation temperature may be possible, which has been limited by the available testing environment.

The temperature error is measured among 10 samples from one processing batch. The sensors were placed along with a

TABLE I
PERFORMANCE SUMMARY AND COMPARISON OF GAN TEMPERATURE SENSORS

Ref.	2013 [15]	2014 [9]	2016 [8]	2020 [16]	This work	
Tech.	GaN IC	GaN IC	GaN 2DEG	GaN SBD	GaN IC (PTAT)	GaN IC (CTAT)
Temp. Range (°C)	25∼250	25∼250	25∼175	25∼200	25∼250	
Supply Voltage (V)	8	12	10	12	8∼60	
Temp. Sensitivity (mV/°C)	−6.5	0.35	10 Ω/°C	0.9∼1.6	15.86	−10.53
Current (μA)	500	216	100	10	70	53
Area (mm^2)	1.23	0.207	N/A	0.2	0.05	

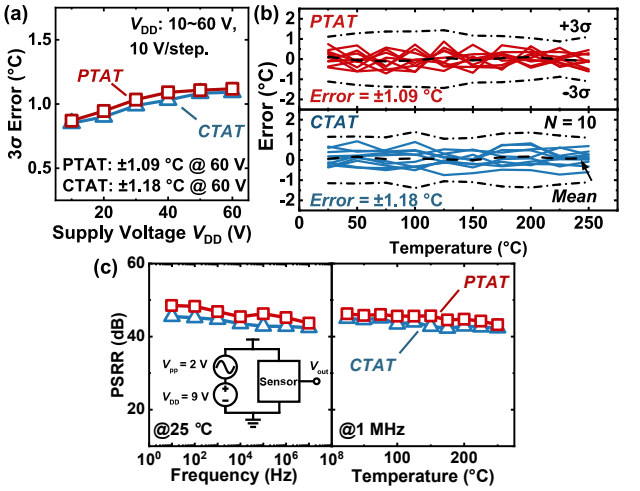

Fig. 6. Measured 3σ temperature error, (a) with supply voltages ranging from 10 V to 60 V (10 V/step), (b) with temperature ranging from 25 to 250 °C at V_{DD} = 60 V. (c) PSRR from 10 Hz to 10 MHz at room temperature and 25 to 250 °C at 1 MHz, with the inset schematic circuit showing the test setup conceptually.

thermocouple calibrated to 50 mK. Fig. 6(a) shows that the errors are less than ±1.2 °C for supply voltages ranging from 10 V to 60 V with 10 V/step. As shown in Fig. 5(b), the maximum 3σ errors are ±1.09 °C for PTAT and ±1.18 °C for CTAT, respectively, when V_{DD} = 60 V. Fig. 6(b) shows the measured temperature error of 10 samples from one processing batch. Meanwhile, the power supply rejection ratio (PSRR) is measured to characterize the power supply variation immunity. As summarised in Fig. 6(c), the PSRR value consistently exceeds 40 dB at various frequencies and temperatures. The low error and high PSRR demonstrate the level of sensing accuracy and robustness.

IV. OVER-TEMPERATURE PROTECTION

The OTP block in integrated GaN power conversion systems ensures system operation safety. This OTP includes a comparator and a PTAT temperature sensor configured in a 2T structure (Fig. 7(a)). It provides a turn-off signal when the chip temperature exceeds the critical temperature T_{set}. The comparator compares the temperature sensing voltage from

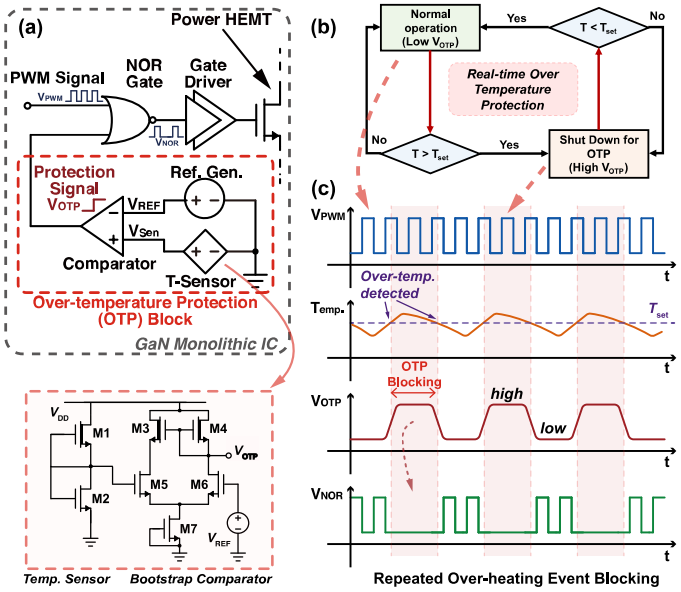

Fig. 7. (a) Schematics of the proposed 2T-based over-temperature protection on GaN power converter circuit. (b) The function block of on-chip over-temperature protection, and (c) timing diagrams of repeated over-heating event blocking.

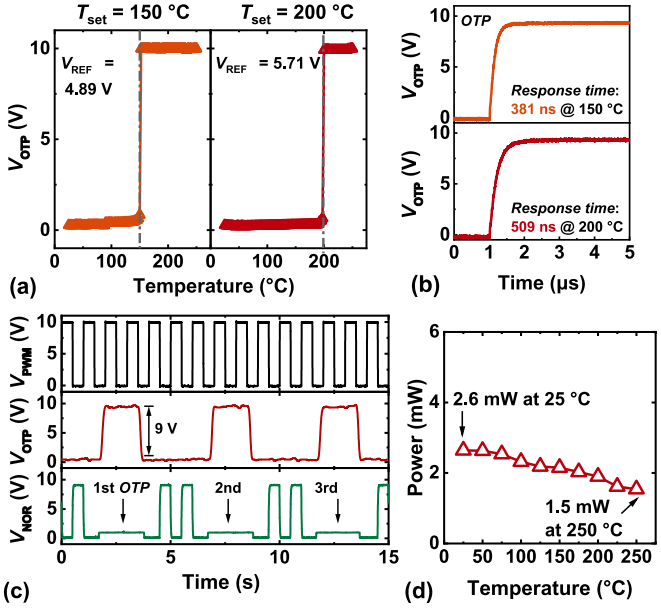

Fig. 8. (a) The OTP output as a function of temperature with various reference voltage V_{REF} with the critical temperature T_{set}, (b) the extracted response times. (c) Waveforms of the OTP at 200 °C and (d) power consumption from 25 to 250 °C, at V_{DD} =10 V.

the sensor with V_{REF}, preset for T_{set}. It triggers the voltage output, V_{OTP}, to change from logic-low to -high when the temperature exceeds T_{set}. The logic module-NOR circuit is used to compare the V_{OTP} with the V_{PWM} and produces a V_{NOR} logic-low output, thereby stop switching of the HEMT (Fig. 7(b), (c)). With the temperature controller of probe station, the temperature rises and falls at rates of 7.5 °C/s and 10 °C/s, respectively.

Fig. 8(a) shows the characteristics of the proposed OTP block. At V_{REF} = 4.89 V, a rapid transition is observed when the temperature sensing detected T_{set} = 150 °C, indicating an over-temperature state. T_{set} can be varied from 150 °C to 200 °C by adjusting V_{REF} to 5.71 V. Variations in process temperature can impact device parameters, and a hysteresis comparator can be employed as a potential solution to determine the appropriate reference voltage V_{REF}. The OTP also exhibits fast start-up, with response times of 381 ns at 150 °C and 509 ns at 200 °C (Fig. 8 (b)), significantly faster than CMOS counterparts with millisecond-level response times [17].

The dynamic characteristics include fast response and a high amplitude output, as shown in Fig. 8(c). When the temperature exceeds the setting temperature 200 °C, the OTP generates a 9 V T_{OTP} signal, serving as a trigger to stop switching directly. Conversely, when temperatures return to normal, the T_{OTP} returns to logic low to resume the switching. The high amplitude OTP output can directly drive the next stage without extra circuits. This feature ensures automatic over-temperature protection for GaN-based circuits. The dynamic characteristics of the OTP could be further improved, which are limited by the speed of the available temperature controller currently.

The OTP power consumption is 2.6 mW at 25 °C and 1.5 mW at 250 °C, as shown in Fig. 8(d). These results highlight the ability of the OTP to prevent the system from thermal damage, demonstrating its potential as a critical component in developing robust and reliable GaN power conversion systems.

V. Conclusion

The monolithic temperature sensor with a compact topology has been realised using GaN MIS-HEMTs. This PTAT/CTAT sensor exhibits stable performance over a wide range of operating voltages and temperatures, and its over-temperature protection is confirmed to be compatible with fast and automatic protection. With its chip-area-efficient structure, the temperature sensing design provides valuable solutions with little overhead for integrating high-performance sensing and protection modules in all-GaN smart power systems.

References

[1] K. J. Chen, O. Häberlen, A. Lidow, C. L. Tsai, T. Ueda, Y. Uemoto, and Y. Wu, "GaN-on-Si power technology: devices and applications," *IEEE Transactions on Electron Devices*, vol. 64, no. 3, pp. 779–795, Mar. 2017, doi: 10.1109/ted.2017.2657579.

[2] E. A. Jones, F. F. Wang, and D. Costinett, "Review of Commercial GaN Power Devices and GaN-Based Converter Design Challenges," *IEEE Journal of Emerging and Selected Topics in Power Electronics*, vol. 4, no. 3, pp. 707–719, Sep. 2016, doi: 10.1109/jestpe.2016.2582685.

[3] D. Reusch and J. Strydom, "Evaluation of Gallium Nitride Transistors in High Frequency Resonant and Soft-Switching DC–DC Converters," *IEEE Transactions on Power Electronics*, vol. 30, no. 9, pp. 5151–5158, Sept. 2015, doi: 10.1109/tpel.2014.2364799.

[4] P. Neudeck, R. Okojie, and L.-Y. Chen, "High-temperature electronics - a role for wide bandgap semiconductors?" *Proceedings of the IEEE*, vol. 90, no. 6, pp. 1065–1076, Jun. 2002, doi: 10.1109/jproc.2002.1021571.

[5] W. Zhang, J. Liang, W. Cui, N. Kim, R. Li, A. Catuneanu, M. Birkett, J. Burgers, and W. Ng, "Compact GaN Power Modules with Direct Bonded Liquid-Cooled Heat Exchanger Suitable for EV Applications," in *2021 IEEE 8th Workshop on Wide Bandgap Power Devices and Applications (WiPDA)*, 2021, pp. 123–128, doi: 10.1109/wipda49284.2021.9645122.

[6] X. Li, T. Pu, L. Li, and J.-P. Ao, "Enhanced Sensitivity of GaN-Based Temperature Sensor by Using the Series Schottky Barrier Diode Structure," *IEEE Electron Device Letters*, vol. 41, no. 4, pp. 601–604, April 2020, doi: 10.1109/led.2020.2971263.

[7] Y. Avenas, L. Dupont, and Z. Khatir, "Temperature Measurement of Power Semiconductor Devices by Thermo-Sensitive Electrical Parameters—A Review," *IEEE Transactions on Power Electronics*, vol. 27, no. 6, pp. 3081–3092, Jun. 2012, doi: 10.1109/tpel.2011.2178433.

[8] R. Reiner, P. Waltereit, B. Weiss, M. Wespel, D. Meder, M. Mikulla, R. Quay, and O. Ambacher, "Linear temperature sensors in high-voltage GaN-HEMT power devices," in *2016 IEEE Applied Power Electronics Conference and Exposition (APEC)*, Mar. 2016, pp. 2083–2086, doi: 10.1109/APEC.2016.7468154.

[9] A. M. H. Kwan, Yue Guan, Xiaosen Liu, and K. J. Chen, "A Highly Linear Integrated Temperature Sensor on a GaN Smart Power IC Platform," *IEEE Trans. Electron Devices*, vol. 61, no. 8, pp. 2970–2976, Aug. 2014, doi: 10.1109/TED.2014.2327386.

[10] D. Yan and D. B. Ma, "A Monolithic GaN Power IC With On-Chip Gate Driving, Level Shifting, and Temperature Sensing, Achieving Direct 48-V/1-V DC–DC Conversion," *IEEE Journal of Solid-State Circuits*, vol. 57, no. 12, pp. 3865–3876, Dec. 2022, doi: 10.1109/jssc.2022.3201781.

[11] Y. Chen and D. B. Ma, "Self-Aging-Prognostic GaN-Based Switching Power Converter Using TJ-Independent Online Condition Monitoring and Proactive Temperature Frequency Scaling," *IEEE Transactions on Power Electronics*, vol. 36, no. 5, pp. 5022–5031, May 2021, doi: 10.1109/tpel.2020.3029450.

[12] D. Reusch, J. Strydom, and J. Glaser, "Improving high frequency DC-DC converter performance with monolithic half bridge GaN ICs," in *2015 IEEE Energy Conversion Congress and Exposition (ECCE)*, 2015, pp. 381–387, doi: 10.1109/ecce.2015.7309713.

[13] M. Cui, Q. Bu, Y. Cai, R. Sun, W. Liu, H. Wen, S. Lam, Y. C. Liang, I. Z. Mitrovic, S. Taylor, P. R. Chalker, and C. Zhao, "Monolithic integration design of GaN-based power chip including gate driver for high-temperature DC–DC converters," *Japanese Journal of Applied Physics*, vol. 58, no. 5, Apr. 2019, doi: 10.7567/1347-4065/ab1313.

[14] A. Li, M. Cui, Y. Shen, Z. Li, W. Liu, I. Z. Mitrovic, H. Wen, and C. Zhao, "Monolithic comparator and sawtooth generator of AlGaN/GaN MIS-HEMTs with threshold voltage modulation for high-temperature applications," *IEEE Transactions on Electron Devices*, vol. 68, no. 6, pp. 2673–2679, Jun. 2021, doi: 10.1109/TED.2021.3075425.

[15] A. M. H. Kwan, Y. Guan, X. Liu, and K. J. Chen, "Integrated Over-Temperature Protection Circuit for GaN Smart Power ICs," *Jpn. J. Appl. Phys.*, vol. 52, no. 8S, p. 08JN15, Aug. 2013, doi: 10.7567/JJAP.52.08JN15.

[16] X. Li, T. Pu, X. Li, L. Li, and J.-P. Ao, "Correlation Between Anode Area and Sensitivity for the TiN/GaN Schottky Barrier Diode Temperature Sensor," *IEEE Trans. Electron Devices*, vol. 67, no. 3, pp. 1171–1175, Mar. 2020, doi: 10.1109/TED.2020.2968358.

[17] H. Wang and P. P. Mercier, "A 763 pW 230 pJ/Conversion Fully Integrated CMOS Temperature-to-Digital Converter With +0.81 °C/-0.75 °C Inaccuracy," *IEEE Journal of Solid-State Circuits*, vol. 54, no. 8, pp. 2281–2290, Aug. 2019, doi: 10.1109/jssc.2019.2916418.